International Journal of Refrigeration (2013) in press

Flow boiling heat transfer of carbon dioxide with polyalkylene glycol–type lubricating oil in pre-dryout region inside horizontal tube

Minxia LI[1], Chaobin DANG[2*], Eiji HIHARA[2]

[1]Key Laboratory of Efficient Utilization of Low and Medium Grade Energy, MOE, Tianjin University, Tianjin, 300072, China

[2]Department of Human and Engineered Environment, Graduate School of Frontier Sciences, The University of Tokyo, 5-1-5 Kashiwanoha, Kashiwa-shi, Chiba 277-8563, Japan

[*]Corresponding author: dangcb@k.u-tokyo.ac.jp; Fax: 81-47-136-4647

ABSTRACT

A flow boiling heat transfer model for horizontal tubes is proposed for CO_2 with entrained polyalkylene glycol (PAG oil) in the pre-dryout region. A general power law–type model with a power number of 3 is used together with the average thermodynamic properties of the CO_2–oil mixture. A convective enhancement factor (F) is recommended according to the relationship between the Lockhart–Martinelli parameter and the ratio α_{tp}/α_{l}, which was obtained based on previous experimental results for CO_2 and oil. A new suppression factor (S) is introduced that comprises a suppression term for forced convection and oil concentration term for bubble generation. A comparison of six correlations showed that the proposed correlation can depict the influence of the mass and heat fluxes on both nucleate and convection boiling reasonably well.

Keywords: Carbon dioxide; heat transfer coefficient; correlation; lubricating oil; boiling heat transfer

Nomenclature

Bo boiling number, $Bo = q/(Gh_{lv})$

c_p specific heat (J kg^{-1} k^{-1})

$E_{l\,mix}$ two-phase heat transfer multiplier

F convective enhancement factor

g gravitational acceleration (m s^{-2})

h_{lv} latent heat of vaporization (J kg^{-1})

m mass flow rate (kg s^{-1})

P_c critical pressure (Pa)

Bd bond number, $Bd = g\rho D^2/\sigma$

D,d hydraulic diameter (m)

EF enhancement factor

Fr Froude number, $Fr = v^2/(gd)$

G mass flux (kg m^{-2} s^{-1})

M molecular weight (kg kmol^{-1})

n total number of data points

Pr Prandtl number $\Pr = \mu/(\rho a)$

p_r reduced pressure $p_r = P/P_c$

q heat flux (W m^{-2})

Re Reynolds number $\mathrm{Re} = Gd/\mu$

S boiling suppression factor

T temperature (°C or K)

T_c critical temperature (K)

T_b oil normal boiling point temperature (K)

x vapor quality

X_{tt} Lockhart–Martinelli parameter

y calculated value

$\bar{y}$ measured value

Greek symbols

α heat transfer coefficient (W m^{-2} K^{-1})

δ film thickness (m)

ε void fraction

θ_{dry} dry angle

λ thermal conductivity (W m^{-1} K^{-1})

μ dynamic viscosity (kg m^{-1} s^{-1})

ν kinematic viscosity (m^2 s^{-1})

ρ density (kg m^{-3})

σ surface tension (N m^{-1})

ω oil concentration (wt%)

Subscripts

b bubble

cal calculated result

cb convective boiling

exp experimental data

l liquid

local local parameter

m refrigerant–lubricant mixture

nb nucleate boiling

o, oil oil

r refrigerant

ref reference

sat saturation

tp two phase

v vapor

w, wall surface

wet wet wall

0 known parameters

1 first parameter

2 second parameter

1. INTRODUCTION

Carbon dioxide (CO_2) was rediscovered by Lorentzen and Pettersen (1993, 1994, 1995) to be a promising alternative refrigerant for heat pump, water heater, and mobile air-conditioning applications because of its favorable properties such as zero ODP (ozone depletion potential), negligible GWP (global warming potential), non-toxicity, and non-flammability. CO_2 also has excellent thermodynamic properties such as low viscosity and surface tension because of its low critical temperature and high operating pressure, which cause it to exhibit unique characteristics in flow and heat transfer. Many previous studies on flow boiling heat transfer of CO_2 (e.g., Pettersen *et al*., 2002, Tanaka and Hihara, 2000, Dang *et al*., 2010) showed that nucleate boiling is the dominant mechanism in CO_2 flow boiling because of the high density ratio of vapor to liquid.

In an actual heat pump cycle, the lubricating oil in the compressor is carried to the other components of the system along with the circulating refrigerant. The entrainment of a small amount of lubricating oil in the refrigerant can cause a profound deterioration in the heat transfer performance of the working fluids. Despite the importance of understanding the behavior of oil inside the CO_2 heat pump cycle, only limited information is available regarding the characteristics of flow boiling heat transfer of CO_2 in the presence of oil. Katsuta *et al*. (2003) measured the boiling heat transfer coefficient of CO_2 in a 3-mm I.D. tube at heat fluxes ranging from 5 to 15 kW m^{-2} and mass fluxes ranging from 200 to 600 kg m^{-2} s^{-1}. A sharp decrease in the heat transfer coefficient was reported when the oil concentration exceeded 0.3%. Gao and Honda (2004a, 2004b) visually observed the flow pattern of lubricating oil flowing with CO_2 at heat fluxes of 5–40 kW m^{-2} and mass fluxes of 230–1200 kg m^{-2} s^{-1}. The formation of an oil-rich layer near the heat transfer surface was reported to be the main cause of the nucleate boiling suppression. Dang *et al*. (2013) presented a systemic experimental study of CO_2 with a polyalkylene glycol (PAG)-type lubricating oil entrained from 0% to 5% in horizontal smooth tubes with inner diameters of 2–6 mm at mass fluxes of 360–1440 kg m^{-2} s^{-1} and heat fluxes of 4.5–36 kW m^{-2}. Experimental results showed that the presence of oil causes the mass flux to significantly influence the heat transfer coefficient at a low heat flux until dryout, while the mass flux was not observed to have a significant influence at a high heat flux.

Shen and Groll (2003) reviewed numerous methods for predicting the heat transfer of a refrigerant in the presence of lubricating oil. However, available literature on predicting the flow boiling heat transfer of CO_2 and oil is limited. Zhao *et al.* (2009) attempted to use two methods to predict the flow boiling coefficient: they chose the correlations of Kandlikar (1990), Liu and Winterton (1991), and Kattan *et al.* (1998) and compared their predictions with the CO_2–lubricant mixture data by replacing the viscosity of pure CO_2 with the viscosity of the mixture. The enhancement factor (*EF*) proposed by Eckels *et al*. (1994, 1998), correlation for R134a/369-SUS and two-phase heat transfer multiplier ($E_{l,mix}$) introduced by Tichy *et al.* (1986), and correlation for R12/300-SUS were applied in these predictions. Zhao *et al.* concluded that an overall prediction based on different correlations is inaccurate, especially under low vapor quality and low oil concentration conditions.

This report presents a prediction model of the flow boiling heat transfer of CO_2–PAG oil mixtures that considers the local properties of a mixture based on the previous experimental work of Dang *et al*. (2013). The proposed correlation and five other available correlations were compared using an experimental database that was set up according to the experimental results of four independent research groups.

2. EXPERIMENTAL APPARATUS AND DATA REDUCTION

The theoretical model is mainly based on previously published experimental results

(Dang *et al*., 2013); a brief description is given here to explain how the data were obtained. Figure 1 shows a schematic diagram of the experimental apparatus. The main devices include a magnetic gear pump to circulate the refrigerant and oil, a mass flow meter (±0.5% accuracy), a heater, an oil sampling section, a test section, an oil separator, and a heat exchanger for cooling the refrigerant. The test section was a stainless steel tube heated electrically by a DC power supply. The outside wall temperature of the test section was measured using T-type thermocouples with an uncertainty of ±0.1 °C. Pressures of the working fluid at the inlet and outlet of the test section were monitored using a precision pressure sensor with an uncertainty of ±0.1% F.S. The vapor quality at the inlet of the test section was controlled by a heater. The oil concentration was measured by the oil sampling section and controlled by the opening of a needle valve at the exit of the oil separator. The oil separator was kept at 60 °C to reduce dissolution of CO_2 into the oil. The sampling was usually conducted three times at the beginning, middle, and end of each run. The uncertainty of the oil concentration was estimated to be ±0.1 %.

The local heat transfer coefficient α was determined from the measured heat flux q and the temperature difference between the saturation temperature T_{sat} and inside wall temperature T_{w}.

$$\alpha = \frac{q}{T_{\mathrm{w}} - T_{\mathrm{sat}}} \tag{1}$$

T_{sat} was estimated from the measured pressure, and T_{w} was calculated from the measured outside wall temperature using a one-dimensional heat conduction model.

The experimental conditions are summarized in Table 1. The thermodynamic properties of CO_2 were obtained from REFPROP 7.0. The measurement accuracies of some parameters are presented in Appendix 1.

3. THEORETICAL ANALYSIS

3.1 Available correlation for CO_2–oil mixture

Most of the CO_2–oil mixture correlations available in the literature were developed based on the properties of pure refrigerants. Katsuta *et al*. (2008a), Gao *et al*. (2008), and Aiyoshizawa *et al*. (2006) proposed correlations to predict the flow boiling heat transfer coefficient of CO_2 and PAG-type oil based on the properties of pure CO_2. The main characteristics of the above models are introduced below. More details on these models are presented in Appendix 2.

Katsuta *et al*. (2008a) and Gao *et al*. (2008) sought to depict the trend of the heat transfer characteristics of the CO_2–oil mixture by revising the boiling suppression factor correlation in the flow boiling heat transfer model for CO_2. Katsuta *et al*. (2008a) proposed their correlation by introducing a new suppression factor into the Stephan–Abdelsalam correlation (Stephan and Abdelsalam, 1980), which reflects the depression on nucleate boiling caused by the presence of oil.

$$\alpha_{\mathrm{nb}} = S\alpha_{SA} \times \phi \tag{2}$$

$$S = \ln\left(2.332\frac{Bo^{0.518}Bd^{1.27}Fr^{0.964}}{\mathrm{Re}_{\mathrm{tp}}^{0.834}}\right) \tag{3}$$

where ϕ is defined as

$$\phi = \frac{1}{\left(1 + OCR^{0.698}Bo^{0.207}Bd^{0.912}\right)} \tag{4}$$

In addition, the factor η, which is the function of the oil concentration, is employed to predict the dryout quality in the presence of oil.

$$\begin{aligned} x_{\mathrm{dry}} &= 0.269 \times \frac{\mathrm{Re}^{0.0571}Fr^{0.0697}}{Bo^{0.0519}}\eta \\ OCR < 1 &\qquad \eta = 1 \\ OCR \geq 1 &\qquad \eta = 1.169e^{-0.17 \times OCR} \end{aligned} \tag{5}$$

The predicted results were reported to agree with 80% of their test results within a prediction deviation of ±20%.

Gao *et al*. (2008) employed Cheng's correlations based on their own experimental data. In their analysis, they redefined suppression factor S' as a function of the vapor quality; the threshold of the vapor fraction was set to 0.7. The correlation was reported to capture 81% of their experimental data within a deviation of ±30%.

$$S' = \begin{cases} S \times \left(-0.5x + 0.35\right) & \left(x \leq 0.7\right) \\ 0 & \left(x > 0.7\right) \end{cases} \tag{6}$$

Considering the suppression of nucleate boiling by flow boiling of CO_2 in the presence of oil, Aiyoshizawa *et al*. (2006) adopted the superposition form of Chen and proposed new constants and exponents for convection enhancement and boiling suppression factor equations based on the previous experimental data of Dang *et al*. (2013). They used the properties of pure CO_2 in their correlation.

$$F = 0.8 + 0.5\left(\frac{1}{X_{tt}}\right)^{1.2} \tag{7}$$

$$S = \frac{1}{6 + \left(\mathrm{Re}_{\mathrm{tp}} \times 10^{-4}\right)^{3}} \tag{8}$$

3.2 Proposed correlation

3.2.1 Properties of CO_2–oil mixture

CO_2 fluid is partly miscible with PAG oil according to Kawaguchi *et al*. (2000) and Kaneko *et al*. (2004). Figure 2 shows the two-phase separation temperature of PAG oil with CO_2

under subcritical conditions (Dang *et al*. 2012). CO_2 and PAG oil separate under the evaporation temperature from -50 °C to 30 °C when the oil concentration is less than 30%. When the oil separates from liquid CO_2, a certain amount of CO_2 may dissolve into the oil. In this study, the inlet oil concentration of the evaporator was below 5%, and the evaporation temperature was kept at 15 °C. Therefore, three phases exist during the evaporation process: a vapor CO_2 phase, liquid CO_2 phase (with negligible dissolved oil), and an oil layer with dissolved CO_2. Based on the experimental measurements of Youbi-Idrissi *et al.* (2003) and Garcia *et al.* (2008), the solubility of CO_2 in PAG oil layer is about 50% when the temperature is 15 °C and pressure is 5.0 MPa.

PAG oil flowing with bulk CO_2 affects both bubble generation on the surface of the tube and the wall superheating temperature. Thermodynamic properties of the oil, such as its viscosity, also influence the flow boiling heat transfer of CO_2. Using just the properties of CO_2 to predict the heat transfer coefficient of the CO_2–oil mixture in the model without considering the contribution of the oil's properties seems unreasonable. In this study, the thermodynamic properties of the CO_2–oil mixture was introduced into the conventional flow boiling heat transfer correlation in order to predict the refrigerant–oil flow boiling coefficient.

The oil concentration in the refrigeration cycle ω_o is defined from the ratio of the mass flow rate of oil to the mass flow of the mixture.

$$\omega_o = \frac{m_{oil}}{m_{co_2} + m_{oil}} \tag{9}$$

Inside the evaporator, the local oil concentration ω_{ol} is the function of the vapor quality and increases with the progress of evaporation:

$$\omega_{ol} = \frac{\omega_o}{1-x} \tag{10}$$

where x is the local vapor quality.

Figure 3 shows that the local oil concentration increases with vapor generation; at an inlet oil concentration ω_o of 1%, ω_{ol} may reach 5 % at a vapor quality of 0.8 and increase sharply at higher vapor quality. However, considering the relatively low dryout quality, which changes from 0.4 to 0.8 based on the mass flux, limiting the scope to low local oil concentrations seems a reasonable constraint.

The average thermal physical properties of CO_2–oil were used in this analysis based on the mixing rules shown in Appendix 3 (Eqs. (A-35)–(A-39)). The thermodynamic properties of PAG used in this study were provided by the manufacturer and are presented in Table 2. The data were correlated as a function of the temperature, as shown in Eqs. (A-40)–(A-43). Table 3 compares the properties of PAG oil, CO_2, and the calculated properties of the CO_2–oil mixture using the mixing rules. Even a tiny amount of entrained oil may lead to a dramatic increase in liquid viscosity and surface tension compared to pure CO_2. At a local oil concentration of 1%, the liquid viscosity and surface tension increase 9.9 and 2.1 times, respectively; when the oil concentration is 5%, these increase 16.9 and 3.6 times, respectively. In contrast, the changes in liquid conductivity, liquid density, and specific heat compared to those of CO_2 are negligible when the oil concentration is small.

The average thermal properties of the mixture defined in this study were applied to calculating the nucleate boiling and force convective heat transfer. For example, the force convection component is given by the following formula:

$$\alpha_{\mathrm{l}} = 0.023\,\mathrm{Re}_{\mathrm{m}}^{0.8}\,\mathrm{Pr}_{\mathrm{m}}^{0.4}\left(\lambda_{\mathrm{m}}/d\right) \tag{11}$$

where $\mathrm{Re}_{\mathrm{m}} = \left[\frac{G(1-x)D}{\mu_{\mathrm{m}}}\right]F^{1.25}$ and subscript "m" denotes the average properties of the mixture being used.

3.2.2 Proposed correlation

Based on the experimental data from Dang *et al.* (2013), a new correlation is proposed. The correlation of Steiner and Taborek (1992) was used in this study; this is a general power law–type model with a power number of 3. The terms for nucleate boiling and convective heat transfer are shown in Eqs. (13) and (14), respectively.

$$\alpha_{\mathrm{tp}} = \left[\left(S\alpha_{\mathrm{nb}}\right)^{3} + \left(\alpha_{\mathrm{cb}}\right)^{3}\right]^{1/3} \tag{12}$$

$$\alpha_{\mathrm{nb}} = 0.00122\left(\frac{\lambda_{\mathrm{m}}^{0.79}\,c_{\mathrm{pm}}^{\;0.45}\,\rho_{\mathrm{m}}^{0.49}}{\sigma_{\mathrm{m}}^{0.5}\,\mu_{\mathrm{m}}^{0.29}\,h_{\mathrm{lv}}^{0.24}\,\rho_{\mathrm{v}}^{0.24}}\right)\left[t_{\mathrm{w}} - t_{\mathrm{sat}}\left(p_{\mathrm{l}}\right)\right]^{0.24}\left[p_{\mathrm{sat}}\left(t_{\mathrm{w}}\right) - p_{\mathrm{l}}\right]^{0.75} \tag{13}$$

$$\alpha_{\mathrm{cb}} = F\alpha_{\mathrm{l}} \tag{14}$$

F and S are defined as

$$F = \begin{cases} 1.0, & X_{\mathrm{tt}} \ge 10 \\ 2.55\left(0.413 + 1/X_{\mathrm{tt}}\right)^{1.05}, & X_{\mathrm{tt}} < 10 \end{cases} \tag{15}$$

$$S = S_{\mathrm{oil}}\frac{1}{0.9 + 0.4\left(\mathrm{Re}_{\mathrm{tpm}}\times 10^{-3}\right)^{0.3} \Big/ \left(\mathrm{Bo}\times 10^{3}\right)^{0.23}} \tag{16}$$

where $\mathrm{Re}_{\mathrm{tpm}} = \left[\frac{G(1-x)D}{\mu_{\mathrm{m}}}\right]F^{1.25}$ and S_{oil} is introduced to reflect the suppression of nucleate boiling due to the presence of oil:

$$S_{\mathrm{oil}} = -\frac{\omega_{\mathrm{ol}}}{2\ln(1-\omega_{\mathrm{ol}})}, 0.0005 \le \omega_{\mathrm{ol}} < 1 \tag{17}$$

3.2.2.1 Discussion of conventional heat transfer component

In general, flow boiling data can be correlated using the form $(\alpha_{\mathrm{tp}}/\alpha_{\mathrm{l}}) \propto (1/X_{\mathrm{tt}})^{n}$, where α_{tp} and α_{l} are the flow boiling heat transfer coefficient and heat transfer coefficient, respectively, for liquid flowing alone and X_{tt} is the Lockhart–Martinelli parameter. Figure 4 shows that the

α_{tp}/α_l regulations of the CO_2–oil mixture and pure CO_2 are similar and not linear to $1/X_{tt}$ in a logarithmic coordinate system. The data of α_{tp} were obtained from Dang *et al*. (2013). When $1/X_{tt}$ and the oil concentration are increased, α_{tp}/α_l of the CO_2–oil mixture deviates from that of pure CO_2. However, the α_{tp}/α_l values of CO_2–oil mixtures with the same oil concentrations under different conditions tend to be identical at high $1/X_{tt}$ values, as shown in Fig. 5.

Figure 6 compares the forced convective heat transfer results from using the mixture properties and those of pure CO_2. The liquid-phase forced convective heat transfer of the mixture is much smaller than that of the pure CO_2 due to the reduction in Re_m with the addition of oil to the refrigerant. The forced heat transfer of the two-phase flow is also affected by the velocity of the vapor and increases with vapor generation. Chen introduced a two-phase multiplier F that relates the ratio of the two-phase Reynolds number to that of the liquid Reynolds number: $F \infty \mathrm{Re}_{tp}/\mathrm{Re}_l$. The Lockhart–Martinelli number is used to calculate F, as shown in Eqs. (18) and (19).

$$F = \begin{cases} 1.0, & X_{tt} \geq 10 \\ 2.0\left(0.213 + 1/X_{tt}\right)^{0.736}, & X_{tt} < 10 \end{cases} \tag{18}$$

$$X_{tt} = \left(\frac{1-x}{x}\right)^{0.9} \left(\frac{\rho_v}{\rho_m}\right)^{0.5} \left(\frac{\mu_m}{\mu_v}\right)^{0.1} \tag{19}$$

Similar to the F factor proposed by Chen (1966), a new definition for the F factor is introduced in Eq. (15) based on the experimental data shown in Fig. 5. In addition, F proposed by Yoshida *et al*. (1994) is shown in Eq. (20) for comparison.

$$F = \begin{cases} 1.0, & X_{tt} \geq 10 \\ 1 + 2.0\left(1/X_{tt}\right)^{0.88}, & X_{tt} < 10 \end{cases} \tag{20}$$

Figure 7 compares the F factors from four correlations (Chen, 1966, Yoshida *et al*., 1994, Aiyoshizawa *et al*., 2006, and the present study). The values of the F factor proposed in this study as calculated by using the mixture's properties were similar to those of the correlations by Yoshida *et al*. and Chen, which were calculated by using the properties of pure CO_2. The F factor of Aiyoshizawa *et al*. (2006) was much lower than that of Chen (1966). Aiyoshizawa *et al*. (2006) apparently tried to decrease the value of F to reflect the suppression of oil. Thus, F was less than 1.0 when the vapor quality was very low, which is physically impossible.

3.2.2.2 Discussion of nucleate boiling component

The nucleate boiling component was constructed using Forster and Zuber's (1955) correlation as modified by Chen (1966), which is shown in Eq. (13).

As noted in Section 3.2.1, three phases exist during the evaporation process: a vapor CO_2 phase, liquid CO_2 phase (with negligible dissolved oil), and oil layer with dissolved CO_2. The proportion of PAG oil dissolved into CO_2 is usually less than 0.2%; its effect on the change in saturation pressure of CO_2 was negligible in our preliminary experiment. Thus, as long as a separate liquid CO_2 phase exists, the saturated temperature of the CO_2–oil mixture is assumed to be equivalent to that that of pure CO_2 and can be determined by the measured local pressure. In addition, the vapor properties used in Eq. (13) are the same as those of pure CO_2. The latent heat of pure CO_2 was used without considering the effect of the oil because the oil concentration was small.

Figure 6 compares the α_{nb} values calculated by Eq. (13) for both pure CO_2 and the CO_2–oil mixture against the vapor quality. α_{nb} of the CO_2–oil mixture decreased with increasing vapor quality due to the change in mixture properties caused by increases in the local oil concentration.

Chen (1966) introduced the factor S to express the suppression of nucleate boiling by convective heat transfer and related it to the two-phase flow Reynolds number as follows:

$$S = \frac{1}{1+\left(2.56\times10^{-6}\right)\left(\mathrm{Re}_{\mathrm{l}}F^{1.25}\right)^{1.17}} \tag{21}$$

As shown in Fig. 5, scattering of $\alpha_{\mathrm{tp}}/\alpha_{\mathrm{l}}$ at low $1/X_{\mathrm{tt}}$ (i.e., low vapor quality) at different heat fluxes showed the contribution of nucleate boiling to heat transfer. At a small mass flux of 360 kg m^{-2} s^{-1}, $\alpha_{\mathrm{tp}}/\alpha_{\mathrm{l}}$ at low vapor quality increased with the heat flux. In addition, $\alpha_{\mathrm{tp}}/\alpha_{\mathrm{l}}$ took similar values at G = 360 kg m^{-2} s^{-1} and q = 9 kW m^{-2} compared to at G = 720 kg m^{-2} s^{-1} and q = 18 kW m^{-2}. The relative significance of nucleate boiling against convective heat transfer in flow boiling heat transfer can be expressed by the boiling number ($Bo = q/(h_{\mathrm{lv}}G)$). Yoshida *et al*. (1994) introduced Bo in their S model as follows:

$$S = \frac{1}{1+0.9\left[\left(\mathrm{Re}_{\mathrm{tp}}\times10^{-4}\right)^{0.5}\Big/\left(\left(Bo\times10^{4}\right)\times X_{\mathrm{tt}}^{\ 0.5}\right)\right]} \tag{22}$$

In this study, a similar expression was proposed based on the experimental data in the presence of oil. The expression of S shown in Eq. (16) considers the suppression of nucleate boiling due to both convective heat transfer and the presence of oil. Since the effect of oil on the nucleate boiling is sophisticated—involving bubble generation suppression, retarded bubble departure, increased surface tension, separation of the oil layer from liquid refrigerant, and the corresponding heat transfer resistance of the oil film—a new factor S_{oil} was introduced into Eq. (16) to reflect all of the other effects that could not be represented by the mixture properties. According to Gao *et al.* (2007), the heat transfer coefficient of a mixture with an oil concentration of less than 0.05% is similar to that of pure CO_2. Therefore, the lower limit for the oil concentration was set to 0.05% in Eq. (17).

Figure 8 compares the four S values. The regulation of S calculated by Eq. (16) and the correlation proposed by Chen (1966) decreased quickly at the beginning and then slowly decline after the vapor reached 0.5. The comparison shows that the proposed S had similar values as the original Chen's model at low vapor qualities. When the vapor quality was increased, the decrease in S of the proposed model was more smooth than that of Chen's model. In contrast, the S values of Aiyoshizawa *et al.*'s model (2006) were much lower than those of the other models because they represented the suppression of nucleate boiling due to the presence of oil by reducing the S value. In addition, the S of Yoshida *et al*.'s model (1994) in Eq. (22) was much higher than that of the other models.

Figure 9 shows the tendencies of the predicted heat transfer coefficient based on the contributions of different constituent terms to the variation in the overall heat transfer coefficient, against the vapor quality. The contribution of nucleate boiling decreased and that of convective heat transfer increased with increasing vapor quality before the onset of dryout. The total heat transfer coefficient (α_{tp}) increased with the mass flux, heat flux, and vapor quality. All of these behaviors were consistent with the regulation based on the experimental results of Dang *et al*. (2013). According to the experimental results, the nucleate boiling and convective heat transfer alternated dominance over the flow boiling at heat transfer under various conditions. At a mass flux of 360 kW m^{-2} s^{-1}, the nucleate boiling term ($S\alpha_{nb}$) increased significantly with the heat flux. At a heat flux of 18 kW m^{-2}, the nucleate boiling and convective heat transfer were dominant in the lower and higher vapor quality regions, respectively. The overall heat transfer coefficient (α_{tp}) was almost constant over the vapor quality range of 0.2–0.8. At a high heat flux of 36 kW m^{-2}, the nucleate boiling term was large and decreased linearly with increasing vapor quality until the vapor quality reached 0.8. At a small heat flux of 4.5 kW m^{-2}, the convective part of the heat transfer coefficient ($F\alpha_l$) dominated almost the entire pre-dryout flow boiling region.

4. COMPARISON of PREDICTED VALUE with EXPERIMENTAL RESULTS

A database was set up based on data from four independent research groups, as listed in Table 4. The database covers experimental data obtained using a mini-channel of 0.86 mm by Zhao *et al.* (2002) to data by Gao *et al.* (2008) using a tube diameter of 3.76 mm. Because Zhao *et al.* (2002) did not explain the type of oil they used, PAG-type oil was considered for this calculation. For the data from Katsuta *et al.* (2008a, 2008b), an average oil concentration was used in the calculation because they presented their groups of measured values for different oil ranges rather than exact oil concentrations. Since the regulation of flow boiling heat transfer observed in the post-dryout region was not similar to that in the pre-dryout region, only the predicted flow boiling heat transfer coefficient in the pre-dryout region was considered in this analysis.

This experimental database was used to compare six prediction methods: namely, the correlations presented by Katsuta *et al*. (2008), Gao *et al*. (2008), Aiyoshizawa *et al*. (2006), Hwang *et al*. (1997), Thome *et al*. (2004), and the newly proposed model. The correlations proposed by Hwang *et al*. (1997) and Thome *et al*. (2004) for pure CO_2 were used, and the mixture properties of CO_2 and oil were applied in these correlations. In contrast, the properties of CO_2 were employed in the correlations of Katsuta *et al*. (2008), Gao *et al*. (2008), and Aiyoshizawa *et al*. (2006) following the original proposal.

In order to compare the accuracies of the prediction methods with the experimental database, the deviation was defined as shown in Eq. (23). Two characteristic parameters were used to provide a global quantitative measure of the performance of the new correlation; their definitions are shown in Eqs. (24) and (25). The relative mean absolute error (RMAE) and relative standard deviation (RSD) in Eqs. (24) and (25) indicate how close the predictions were to the eventual outcomes.

Deviation

$$\mathrm{ED} = \frac{y_{\mathrm{exp}} - y_{\mathrm{cal}}}{y_{\mathrm{exp}}} \tag{23}$$

Relative mean absolute error

$$\mathrm{RMAE} = \frac{1}{n}\sum_{i=1}^{n}\left|\frac{y_{\mathrm{exp,i}} - y_{\mathrm{cal,i}}}{y_{\mathrm{exp,i}}}\right| \tag{24}$$

Relative standard deviation

$$\mathrm{RSD} = \sqrt{\frac{\sum_{i=1}^{n}\left(\left|\frac{y_{\mathrm{exp,i}} - y_{\mathrm{cal,i}}}{y_{\mathrm{exp,i}}}\right| \text{-RMAE}\right)^2}{n-1}} \tag{25}$$

Figure 10 shows the previous experimental results (Dang *et al*., 2013, Katsuta *et al*., 2008a, 2008b, Gao *et al*., 2007, 2008) for CO_2 with a small amount of lubricating oil and the prediction results of the new correlations. Figure 10(a) shows that the results predicted by the newly proposed correlation illustrated similar regulations at different oil concentrations with increasing vapor quality. However, the oil concentration affected the calculated heat transfer coefficient more significantly than that indicated by the experimental results. Aiyoshizawa *et al*.'s (2006) results were independent of the oil concentration and did not reflect the influence of oil on the heat transfer. Figures 10(b) and (c) show that the prediction by the newly proposed correlation tended to be similar to the experimental values of Katsuta *et al*. (2008a) and Gao *et al*. (2007), and the prediction results reflected the regulation of the effect of the oil concentration on the heat transfer coefficients.

Figure 11(a) compares the predicted and measured heat transfer coefficients in a 2-mm I.D. tube with an oil concentration of 1% and mass flux of 360 kg m^{-2} s^{-1} to demonstrate the effect of the heat flux based on the data of Dang *et al*. (2013). The heat flux had a strong positive influence on the heat transfer coefficient for a majority of the vapor quality region when the heat flux was increased from 4.5 kW m^{-2} to 36 kW m^{-2}, and the mass flux stayed at 360 kg m^{-2}

s^{-1}. The theoretical results predicted by the newly proposed correlation depicted the characteristics of the heat transfer coefficient well: they showed the tendency of the heat transfer coefficients against the vapor quality to change from an upward movement to a downward movement when the heat flux rose and the mass flux remained constant. At heat fluxes of 4.5 and 9 kW m^{-2}, the theoretical heat transfer coefficients from the newly proposed correlation matched the measurements well at low vapor quality and gradually deviated from the experimental coefficients at high vapor quality. For both the heat fluxes, the predicted results tended to increase with the vapor quality in the pre-dryout region. This shows the strong influence of convective boiling on the heat transfer coefficients. At a heat flux of 18 kW m^{-2}, both the measured pre-dryout heat transfer coefficients and the prediction by the new proposed correlation barely changed with variations in the vapor quality. The nucleate boiling was considered to be the dominant mechanism affecting the contribution of the heat transfer coefficient to the flow boiling of CO_2. When the heat flux was increased to 36 kW m^{-2}, the theoretical heat transfer coefficient decreased steadily with increasing vapor quality and matched the dynamics of the measured results well. The prediction results from the correlation of Aiyoshizawa *et al*. (2006) increased with the heat flux and vapor quality. However, the tendencies of some prediction data were different from those of the experimental results when the heat flux reached 18 kW m^{-2} and especially 36 kW m^{-2}.

Figure 11(b) compares the measured and calculated results for a CO_2–oil mixture at a heat flux of 18 kW m^{-2}, mass flux of 360–1440 kg m^{-2} s^{-1}, and oil concentration of 1%. In Fig. 11(b), both the theoretical and experimental heat transfer coefficients showed that the mass flux had a positive influence on the heat transfer coefficient of the CO_2–oil mixture in the pre-dryout region; this differs from the case under oil-free conditions. Under oil-free conditions, the heat transfer coefficient with a large mass flux was slightly lower than that with a small mass flux (Dang *et al*., 2010). The difference was attributed to the suppression of nucleate boiling due to oil entrainment. In oil-free CO_2, the density difference between the liquid and vapor phases is very small; thus, nucleate boiling is predominant for the overall heat transfer coefficient compared to convective heat transfer. However, the presence of oil retards bubble generation and bubble departure due to the increased surface tension and liquid viscosity, which suppresses nucleate boiling. The convective heat transfer of the CO_2–oil mixture thus becomes prominent. The values predicted by the new proposed correlation almost matched the trend of the measured data. When the mass flux was 360 kg m^{-2} s^{-1}, the nucleate boiling and convective heat transfer were comparable, and the heat transfer coefficients showed a gentle tendency with an increase in vapor quality. When the mass flux was increased to 720 and 1440 kg m^{-2} s^{-1} at a heat flux of 18 kW m^{-2}, the influence of the dominant convective heat transfer caused the heat transfer coefficient to increase with the vapor quality.

Figures 12(a)–(d) compare the measured and calculated flow boiling heat transfer coefficients of the CO_2–oil mixture using the above correlations. The comparisons showed that the best-fitting correlations were those of Aiyoshizawa *et al*. (2006) and the proposed model, which were based on almost the same experimental results. These correlations were in good agreement with approximately 95% of the data of Dang *et al*. (2013) and also corroborated about 90% of the data of Gao *et al*. (2007, 2008) and approximately 70% of the data of Katsuta *et al*. (2008a, 2008b) within a deviation of ±30%. Because of the smaller inner diameter of the test tube (0.86 mm) used by Zhao *et al*. (2002) and the unknown oil type, the prediction deviations of these two correlations are large. The correlations proposed by Katsuta *et al*. (2008) and Gao *et al*. (2008) partially corroborated the data from Dang *et al*. (2013), Gao *et al*. (2007, 2008), and Katsuta *et al*. (2008a, 2008b). Table 5 presents the RMAE and RSD of the six correlations. The correlations of Hwang *et al*. (1997) and Thome *et al*. (2004) for pure CO_2, when used with the properties of the mixture, could not obtain acceptable deviations. The correlations for pure CO_2 must therefore be corrected before they can be utilized to predict the heat transfer coefficient of a CO_2–oil mixture. The correlations of the proposed model and Aiyoshizawa *et al*. (2006) outperformed the other correlations in terms of predicting the flow boiling heat transfer of the CO_2–oil mixture. The main differences between these two correlations were that the proposed model considered the properties of the mixture during calculation and provided superior performance when based on the measured results of Dang *et al*. (2013).

5. CONCLUSIONS

This paper proposed a prediction model for the flow boiling heat transfer of CO_2 with a small amount of PAG-type lubricating oil. The main conclusions are as follows:

(1) A prediction model for the heat transfer coefficient is proposed that considers the properties of the CO_2–oil mixture using new F and S factors. The proposed F factor with the mixture properties is similar to that proposed for pure refrigerant. Factor S was revised by introducing factor S_{oil} to consider the influence of oil on nucleate boiling.

(2) The proposed correlation matched most (95%) of the experimental results of Dang *et al*. (2013) with a deviation of ±30%. It also matched 90% of the data from Gao *et al*. (2007, 2008) within a deviation of ±30%.

(3) Based on this model, increasing the oil concentration causes a gentle decrease in the predicted heat transfer coefficient of a CO_2–oil mixture.

(4) The proposed correlation can describe the tendency of the heat transfer coefficient of a CO_2–oil mixture at various heat and mass fluxes and agrees well with the experimental results.

ACKNOWLEDGMENTS

The authors express their gratitude to Panasonic Corp. for their financial support. The first author is grateful for the support of the JSPS and NSFC No. 50976075.

REFERENCES

Aiyoshizawa, K., Yamada, T., Haraguchi, N., Dang, C., Hihara E., 2006. The influence of lubricating oil on boiling heat transfer characteristics of carbon dioxide in horizontal smooth tubes. Proceedings of the 43rd National Heat Transfer Symposium of Japan, Nagoya, July 31-June 2, CD-G133.

Chen, J.C., 1966. Correlation for boiling heat transfer to saturated fluids in convective flow. Ind. Eng. Chem. Res. 5(3), 322–339.

Cheng, L., Ribatski, G., Wojtan, L., Thome, J. R., 2006. New flow boiling heat transfer model and flow pattern map for carbon dioxide evaporating inside horizontal tubes. Int. J. Heat Mass Transfer, 49, 4082–4094.

Conde, M.R., 1996. Estimation of thermophysical properties of lubricating oils and their solution with refrigerants: An appraisal of existing methods. Appl. Therm. Eng. 16(1), 51-61.

Dang, C., Haraguchi, N., Yamada, T., Hihara, E., 2006. Boiling heat transfer of carbon dioxide in a horizontal tube. International Heat Transfer Conference IHTC-13, Sydney, Australia, Aug.

Dang, C., Haraguchi, N., Hihara, E., 2010. Flow boiling heat transfer of carbon dioxide inside a small-sized microfin tube, Int. J. Refrig. 33, 655-663.

Dang, C., Hoshika, K., Hihara, E., 2012. Effect of lubricating oil on the flow and heat transfer characteristics of supercritical carbon dioxide, Int. J. Refrig. 35, 1410-1417.

Dang, C., Haraguchi, N., Yamada, T., Li, M., Hihara, E., 2013. Effect of lubricating oil on flow boiling heat transfer of carbon dioxide, Int. J. Refrig. 36, 136-144.

Eckels, S.J., Doerr, T.M., Pate, M.B., 1998. A comparison of the heat transfer and pressure drop performance of R134a–lubricant mixtures in different diameter smooth tubes and micro-fin tubes. ASHRAE Trans. 104, (Part 1A) 376–386.

Eckels, S.J., Doerr, T.M., Pate, M.B., 1994. In-tube heat transfer and pressure drop of R-134a and ester lubricant mixtures in a smooth tube and a micro-fin tube. Part I. Evaporation, ASHRAE Trans. 100, 265–282.

Gao, L., Honda, T., 2004a. Boiling heat transfer characteristics of CO_2 in a horizontal thin tube. Proc. of the 2004 JSRAE Annual Conference, Matsuhama, Japan: Japan Society of Refrigeration and Air Conditioning Engineers, Oct, B110.

Gao, L., Honda, T., 2004b. Observation of the flow of refrigerant and lubricating oil in a CO_2 heat pump system. Proc. of the 2004 JSRAE Annual Conference, Matsuhama, Japan: Japan Society of Refrigeration and Air Conditioning Engineers, Oct, B108.

Gao, L., Honda T., Koyama S., 2007. Experiments on flow boiling heat transfer of almost pure CO_2 and CO_2-Oil mixtures in horizontal smooth and microfin tubes HVAC&R Res. 13(3), 415–425.

Gao, L., Matsusaka Y., Sato M., Honda T., 2008. Correlations of evaporation heat transfer of CO_2-PAG oil mixtures in a horizontal smooth tube, Proceedings of the 2008 JSRAE Annual Conference, Osaka, Japan: Japan Society of Refrigeration and Air Conditioning Engineers, Oct. 20–23, C142, 279–282.

Garcia, J., Youbi-Idrissi, M., Bonjourc, J., Fernandez, J. 2008, Experimental and PC-SAFT volumetric and phase behavior of carbon dioxide + PAG or POE lubricant systems, J. of Supercritical Fluids, 47, 8–16.

Forster, H.K., Zuber, N., 1955. Dynamics of vapor bubbles and boiling heat transfer, AIChE J. 531–535.

Hwang, Y., Kim, B., Radermacher, R., 1997. Boiling heat transfer correlation for carbon dioxide. Proceedings of International Conference on Heat Transfer Issues in Natural Refrigerant, College Park, 44–57.

Ikeda, H., Kaneko, M., Tokiai, T., Yoshii, A., Suto, H., 2006. Evaluation of lubricants for a carbon dioxide automobile A/C system, SAE 7th Alternate Refrigerant Systems Symposium June 29th.

Kandlikar, S.G., 1990. A general correlation for two-phase flow boiling horizontal and vertical tubes. J. Heat Transfer. 112, 219–228.

Katsuta, M., Kinpara, H., Aoyagi, T., Yagi, S., Mukaiyama, H., Kamimura, I., 2003. Evaporative heat transfer characteristics of CO_2 refrigeration cycle and comparison with R134a—The change of thermal and hydraulic characteristics due to evaporation temperature. Proc. of the 2003 JSRAE Annual Conference, Tokyo, Japan: Japan Society of Refrigeration and Air Conditioning Engineers, Oct, A309.

Katsuta, M., Okuma, K., Hirade, T., Miyachi, N., 2008a. The effect of lubricating oil fraction rate on the CO_2 evaporating thermal and hydraulic characteristics, International Refrigeration and Air Conditioning Conference at Purdue, 2008–2209.

Katsuta, M., Kishi, S., Miyachi, N., Oshiro, T., 2008b. Evaporating heat transfer characteristics of R744 - Flow visualization of oil contaminated CO_2 two-phase flows and a discussion focused on its transition, Proceedings of the 2008 JSRAE Annual Conference, Osaka, Japan: Japan Society of Refrigeration and Air Conditioning Engineers, Oct. 20–23, C133, 267–270.

Kattan, N., Thome, J.R., Favrat, D., 1998. Flow boiling in horizontal tube. Part III. Development of a new heat transfer model based on flow pattern, J. Heat Transfer. 120, 156–165.

Kawaguchi, Y., Takesue, M., Kaneko, M., Tazaki, T., 2000. Performance study of refrigerating oils with CO_2. 2000 SAE Automotive Alternative Refrigerant System Symposium, Scottsdale, AZ.

Kaneko, M., Ikeda, H., Kawaguchi, Y., 2004. The development of capped-PAG refrigeration lubricants for automotive A/C with CO_2 and HFC152a. 2004 SAE Automotive Alternative

Refrigerant System Symposium, Scottsdale, AZ.
Liley, P.E., Gambill, W.R., 1973. Physical and chemical data. In: Perry, Chilton, editors. Chemical Engineering Handbook, 5^{th} ed. New York.
Liu, Z., Winterton, R.H.S., 1991. A general correlation for saturated and subcooled flow boiling in tubes and annuli based on a nucleate pool boiling equation, Int. J. Heat Mass Transfer. 34, 2759–2766.
Lorentzen, G., Pettersen, J., 1993. A new efficient and environmentally benign system for car air-conditioning. Int. J. Refrig. 16(1), 4–12.
Lorentzen, G., 1994. Revival of carbon dioxide as a refrigerant. Int. J. Refrig. 17(5), 292–301.
Lorentzen, G., 1995. The use of natural refrigerants: a complete solution to the CFC/HCFC predicament. Int. J. Refrig. 18(3), 190–97.
Pettersen, J., Rieberer, R., Munkejord, S.T., 2000. Heat transfer and pressure drop characteristics of evaporating carbon dioxide in micro-channel tubes. Preliminary Proceedings of the 4th IIR-Gustav Lorentzen Conference on Natural Working Fluids at Purdue, 107-114.
REFPROP. NIST Standard Reference Database 23, Version 7.0.
Robbins, L.A., Kingrea, C.L., 1962. Hydrocarbon Proc. Petrol Ref. 41(5), 133.
Shen, B., Groll, A., 2003. Critical literature review of lubricant influence on refrigerant heat transfer and pressure drop. Final Report, ARTI-21CR/611-20080.
Steiner, D., Taborek, J., 1992. Flow boiling heat transfer in vertical tubes correlated by an asymptotic model. Heat Transfer Eng. 13, 43–89.
Stephan, K., Abdelsalam,M., 1980. Heat transfer correlation for natural convection boiling, Int. J. Heat Mass Transfer. 23, 73–87.
Tichy, J.A., Duval, W.M.B., Macken, N.A., 1986. Experimental investigation of heat transfer in forced-convection evaporation of oil–refrigerant mixtures. ASHRAE Trans. 92 (Part II), 450–460.
Thome, J.R., Hajal, J. El, 2004. Flow boiling heat transfer to carbon dioxide: general prediction method, Int. J. Refrig. 27, 294–301.
Youbi-Idrissi, M., Bonjour, J., Terrier, M.F., Meunier, F., 2003, Solubility of CO_2 in a synthetic oil, in: Proceedings of 21st International Congress of Refrigeration, Washington, DC, pp. 1–9.
Yoshida, S., Mori, H., Hong, H., Matsunaga, T., 1994. Prediction of heat transfer coefficient for refrigerants flowing in horizontal evaporator tubes. Trans. of the JAR. 11(1), 67–78.
Zhao, X., Bansal, P., 2009. Critical review of flow boiling heat transfer of CO_2-lubricant mixtures. Int. J. Heat Mass Transfer. 52, 870–879.
Zhao, Y., Molki, M., Ohadi, M.M., Fanca, F.H.R., Radermacher, R., Cho, K., 2002. Flow boiling of CO_2 with miscible oil in microchannels. ASHRAE Trans. 108(1), 135–144.

Appendix 1

Measured accuracy of the parameters in the experiment of Dang *et al*. (2013)

Item	Uncertainties
oil concentration (ω_o)	0.1%
Heat flux (q_w)	±3%
T_w	±0.1 °C
T_{sat}	±0.03 °C
Vapor fraction	±3.3%
Heat transfer coefficient (α)	From ±8.9% to ±13%.

Appendix 2

1) Correlation of Hwang *et al*. (1997) for pure CO_2

$$\alpha_{tp} = \alpha_{nb} + \alpha_{cb} \tag{A-1}$$

$$\alpha_{nb} = 0.00122 S \left(\frac{\lambda_l^{0.79} c_{pl}^{0.5} \rho_l^{0.49}}{\sigma^{0.6} \mu_l^{0.29} h_{lv}^{0.24} \rho_v^{0.24}} \right) \left[t_w - t_{sat}\left(p_l\right) \right]^{0.4} \left[p_{sat}\left(t_w\right) - p_l \right]^{0.75} \tag{A-2}$$

$$S = \frac{1-\exp(-F\alpha_l\ X\ /\lambda_l)}{F\alpha_l\ X\ /\lambda_l}, X = 0.05\left(\frac{\sigma}{g(\rho_l - \rho_v)} \right)^{0.5} \tag{A-3}$$

$$\alpha_{cb} = \alpha_l F \, \mathrm{Pr}_l^{0.6}, \quad \alpha_l = 0.023 \, \mathrm{Re}_l^{0.8} \, \mathrm{Pr}_l^{0.4} \left(\lambda_l / d \right) \tag{A-4}$$

$$F = 1.0, X_{tt} \geq 10 \tag{A-5}$$

$$F = 2.0 \left(0.213 + 1/X_{tt} \right)^{0.736}, X_{tt} < 10 \tag{A-6}$$

$$X_{tt} = \left(\frac{1-x}{x} \right)^{0.9} \left(\frac{\rho_v}{\rho_l} \right)^{0.5} \left(\frac{\mu_l}{\mu_v} \right)^{0.1} \tag{A-7}$$

2) Correlation of Thome *et al*. (2004) for pure CO_2

$$\alpha_{tp} = \frac{d\theta_{dry}\alpha_v + d\left(2\pi - \theta_{dry}\right)\alpha_{wet}}{2\pi d} \tag{A-8}$$

$$\alpha_{wet} = \left[\left(S\alpha_{nb,CO_2} \right)^3 + \alpha_{cb}^3 \right]^{1/3} \tag{A-9}$$

$$\alpha_{\mathrm{nb}} = 55 p_r^{0.12} \left(-\log_{10} p_r\right)^{-0.55} M^{-0.5} q^{0.67} \tag{A-10}$$

$$\alpha_{\mathrm{cb}} = 0.0133 \left(\frac{4G(1-x)\delta}{(1-\varepsilon)\mu_{\mathrm{l}}} \right)^{0.69} \left(\frac{c_{\mathrm{pL}} \mu_{\mathrm{l}}}{\lambda_{\mathrm{l}}} \right)^{0.4} \frac{\lambda_{\mathrm{l}}}{\delta} \tag{A-11}$$

$$\alpha_{\mathrm{v}} = 0.023 \left(\frac{Gxd}{\varepsilon \mu_{\mathrm{v}}} \right)^{0.8} \left(\frac{c_{\mathrm{pv}} \mu_{\mathrm{v}}}{\lambda_{\mathrm{v}}} \right)^{0.4} \frac{\lambda_{\mathrm{v}}}{d} \tag{A-12}$$

$$\alpha_{\mathrm{nb,CO_2}} = 0.71 \alpha_{\mathrm{nb}} + 3790 \tag{A-13}$$

$$S = \frac{(1-x)^{1/2}}{0.121 \mathrm{Re}_{\mathrm{l}}^{0.225}} \tag{A-14}$$

$$\varepsilon = \frac{x}{\rho_{\mathrm{v}}} \left[\left(1 + 0.12(1-x)\right) \left(\frac{x}{\rho_{\mathrm{v}}} + \frac{1-x}{\rho_{\mathrm{l}}} \right) + \frac{1.18}{G} \left(\frac{g\sigma(\rho_{\mathrm{l}} - \rho_{\mathrm{v}})}{\rho_{\mathrm{l}}^2} \right)^{1/4} (1-x) \right]^{-1} \tag{A-15}$$

3) The correlations of Gao *et al*. (2008) are the same as those of Cheng *et al*. (2006) except for additional suppression factors for the CO_2–oil mixture.

$$\alpha_{\mathrm{tp}} = \left[(S\alpha_{\mathrm{nb}})^3 + \alpha_{\mathrm{cb}}{}^3 \right]^{1/3} \tag{A-16}$$

$$S' = \begin{cases} S \times (-0.5x + 0.35) & (x \le 0.7) \\ 0 & (x > 0.7) \end{cases} \tag{A-17}$$

4) Correlation of Katsuta *et al*. (2008b) for CO_2–oil mixture

$$\alpha_{\mathrm{tp}} = \alpha_{\mathrm{nb}} + \alpha_{\mathrm{cb}} \tag{A-18}$$

$$\alpha_{\mathrm{cb}} = F \times 0.023 \frac{\lambda_{\mathrm{l}}}{D} \left(\frac{G(1-x)D}{\mu_{\mathrm{l}}} \right)^{0.8} \mathrm{Pr}^{0.4} \tag{A-19}$$

$$F = 1 + 0.258 \times \left(\frac{1}{X_{tt}} \right)^{0.886} + 92.32 \left(\frac{\rho_{\mathrm{v}}}{\rho_{\mathrm{l}}} \right)^{3} \left(\frac{1}{X_{tt}} \right)^{0.9} \tag{A-20}$$

$$\alpha_{\mathrm{nb}} = S \alpha_{SA} \times \phi \tag{A-21}$$

$$\alpha_{SA} = 207 \frac{\lambda_l}{D_b} \left(\frac{q D_b}{\lambda_l T_{sat}} \right)^{0.745} \left(\frac{\rho_v}{\rho_l} \right)^{0.581} \mathrm{Pr}_l^{0.533} \tag{A-22}$$

$$S = \ln\left(2.332 \frac{Bo^{0.518} Bd^{1.27} Fr^{0.964}}{\mathrm{Re}_{tp}^{0.834}} \right) \tag{A-23}$$

$$\phi = \frac{1}{\left(1 + OCR^{0.698} Bo^{0.207} Bd^{0.912}\right)} \tag{A-24}$$

$$x_{dry} = 0.269 \times \frac{\mathrm{Re}^{0.0571} Fr^{0.0697}}{Bo^{0.0519}} \tag{A-25}$$

$$OCR < 1 \quad \eta = 1 \tag{A-26}$$

$$OCR \geq 1 \quad \eta = 1.169 e^{-0.17 \times OCR} \tag{A-27}$$

5) Correlation of Aiyoshizawa *et al*. (2005)

$$\alpha_{tp} = F\alpha_{cb} + S\alpha_{nb} \tag{A-28}$$

$$\alpha_{cb} = 0.023 \frac{\lambda_l}{d} \left[\frac{G(1-x)d}{\mu_l} \right]^{0.8} \mathrm{Pr}^{0.4} \tag{A-29}$$

$$\alpha_{nb} = 207 \frac{\lambda_l}{\mathrm{D_b}} \left(\frac{q D_b}{\lambda_l T_b} \right)^{0.745} \left(\frac{\rho_v}{\rho_l} \right)^{0.581} \mathrm{Pr}_l^{0.533} \tag{A-30}$$

$$D_b = 0.51 \left[\frac{2\sigma}{g(\rho_l - \rho_v)} \right]^{0.5} \tag{A-31}$$

$$\mathrm{Re}_{tp} = \left[\frac{G(1-x)D}{\mu_l} \right] F^{1.25} \tag{A-32}$$

$$F = 0.8 + 0.5 \left(\frac{1}{X_{tt}} \right)^{1.2} \tag{A-33}$$

$$S = \frac{1}{6 + \left(\mathrm{Re}_{tp} \times 10^{-4}\right)^3} \tag{A-34}$$

Appendix 3

$$\rho_{\mathrm{m}} = \rho_{\mathrm{o}} \cdot \omega_{\mathrm{ol}} + \rho_{\mathrm{r}} \cdot \left(1-\omega_{\mathrm{ol}}\right) \tag{A-35}$$

$$\ln \nu_{\mathrm{m}} = \omega_{\mathrm{ol}} \ln \nu_{\mathrm{o}} + \left(1-\omega_{\mathrm{ol}}\right) \ln \nu_{\mathrm{r}} \tag{A-36}$$

$$c_{\mathrm{pm}} = (1-\omega_{\mathrm{ol}}) c_{\mathrm{pr}} + \omega_{\mathrm{ol}} c_{\mathrm{po}} \tag{A-37}$$

$$\sigma_{\mathrm{m}} = \sigma_{\mathrm{r}} + \left(\sigma_{\mathrm{o}} - \sigma_{\mathrm{r}}\right)\sqrt{1-\omega_{\mathrm{r}}} \tag{A-38}$$

$$\lambda_{\mathrm{m}} = \lambda_{\mathrm{r}}\omega_{\mathrm{r}} + \lambda_{\mathrm{o}}\left(1-\omega_{\mathrm{r}}\right) - 0.72\left(1-\omega_{\mathrm{r}}\right)\omega_{\mathrm{r}}\left(\lambda_{\mathrm{o}} - \lambda_{\mathrm{r}}\right) \tag{A-39}$$

Conde (1996) presented an equation to predict the density of oil against temperature:

$$\rho(T) = \rho_0(T) - A(T_0 - T) \tag{A-40}$$

where T_0 is a reference temperature and was taken as 15 °C here; $\rho_0(T_0)$ is the density at the reference temperature (kg m^{-3}); and $A = 0.8$ for the oil proposed by Conde.

Liley *et al.* (1973) proposed a formula to calculate the specific heat:

$$C_{\mathrm{p}} = \frac{4.1861}{\sqrt{S_0}}\left[0.388 + 0.00045\left(\frac{9}{5}t + 32\right)\right] \tag{A-41}$$

where S_0 is the relative density. $S_0 = \rho_{\mathrm{o}}/\rho_{\mathrm{w}}$, which is the ratio of the liquid density and pure water density (999.0 kg m^{-3} at a temperature of 15 °C).

Robbins and Kingrea (1962) proposed a correlation to calculate the conductivity of a fluid as a function of the molecular weight, density, specific heat, and critical temperature.

$$\lambda = \frac{\Delta_1}{M^{1/2}} \frac{3 + 20\left(1 - \dfrac{T}{T_{\mathrm{c}}}\right)^{2/3}}{3 + 20\left(1 - \dfrac{T_{\mathrm{sb}}}{T_{\mathrm{c}}}\right)^{2/3}} \tag{A-42}$$

where $\Delta_1 = 1.5$ for lubricants. T_{sb} and T_{c} are the standard boiling point and critical temperature, respectively, of PAG oil (K) as shown in Table 2. Based on the data in Table 2, the maximum deviation between the properties calculated by Eq. (A-42) and those provided by the manufacturer of the oil is less than ±5%.

The viscosity of PAG oil is correlated to the temperature in the following function:

$$\lg(\lg(\nu + A)) = B \lg T + C \tag{A-43}$$

where A, B, and C have recommended values of 0.6, 2.468, and 6.46, respectively, to best fit the viscosity data given in Table 2.

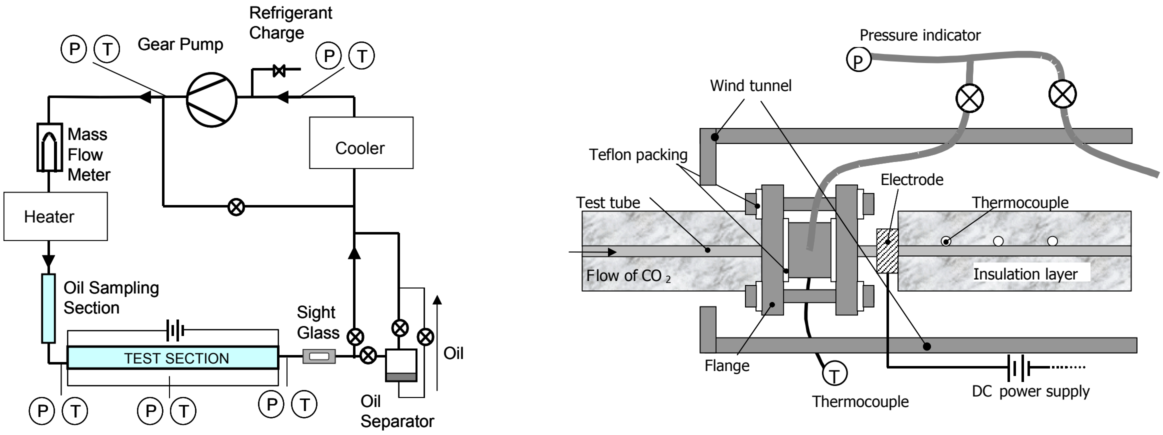

(a) Experimental system (b) Detailed structure of test section

Figure 1 Schematic diagram of experimental apparatus.

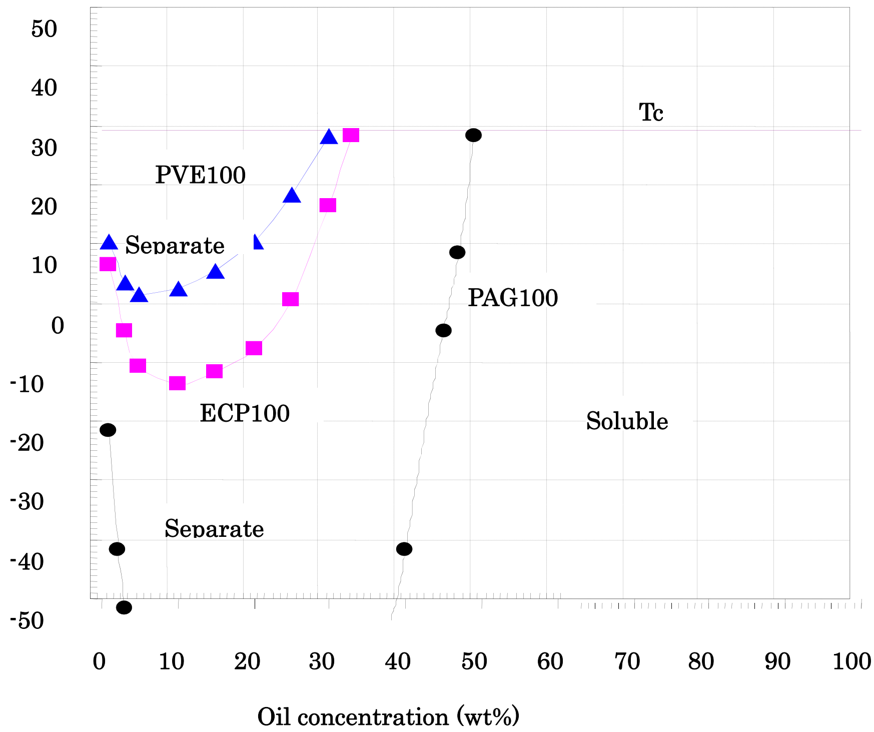

Figure

2 Two-phase separation temperature.

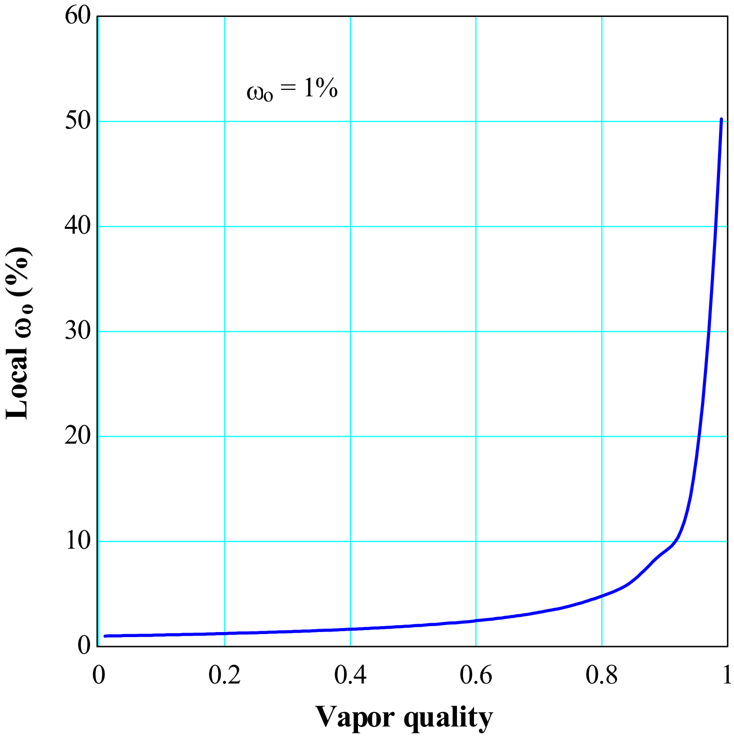

Figure 3 Variation in local oil concentration against vapor quality.

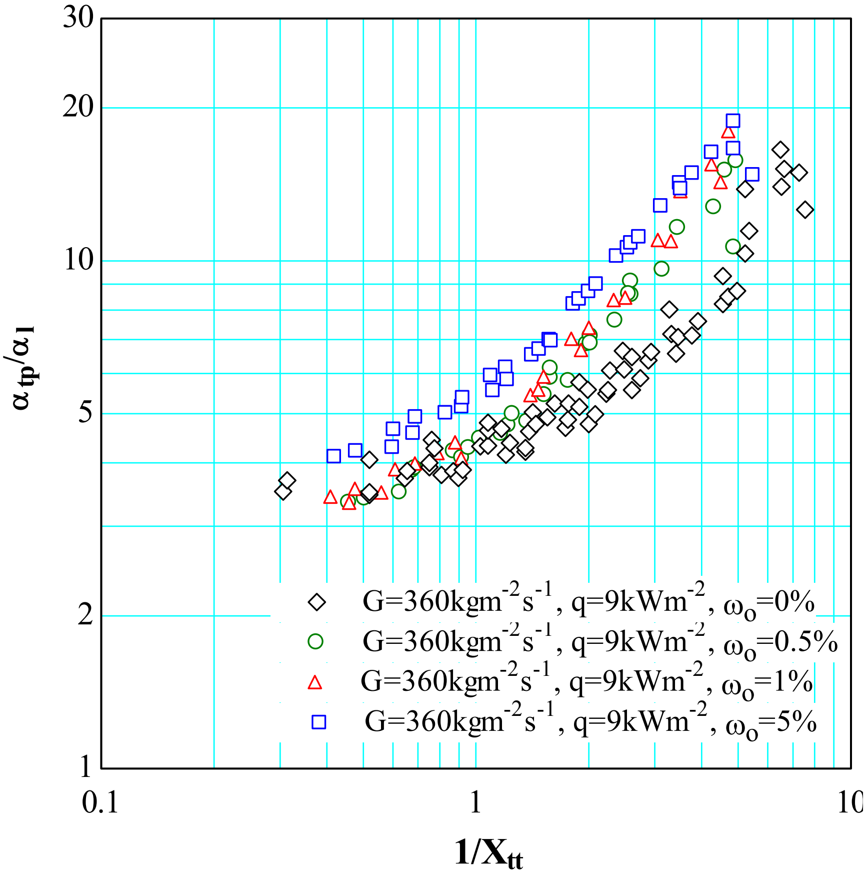

Figure 4 Variation in boiling heat transfer coefficient ratio at various oil concentrations against Lockhart–Martinelli parameter.

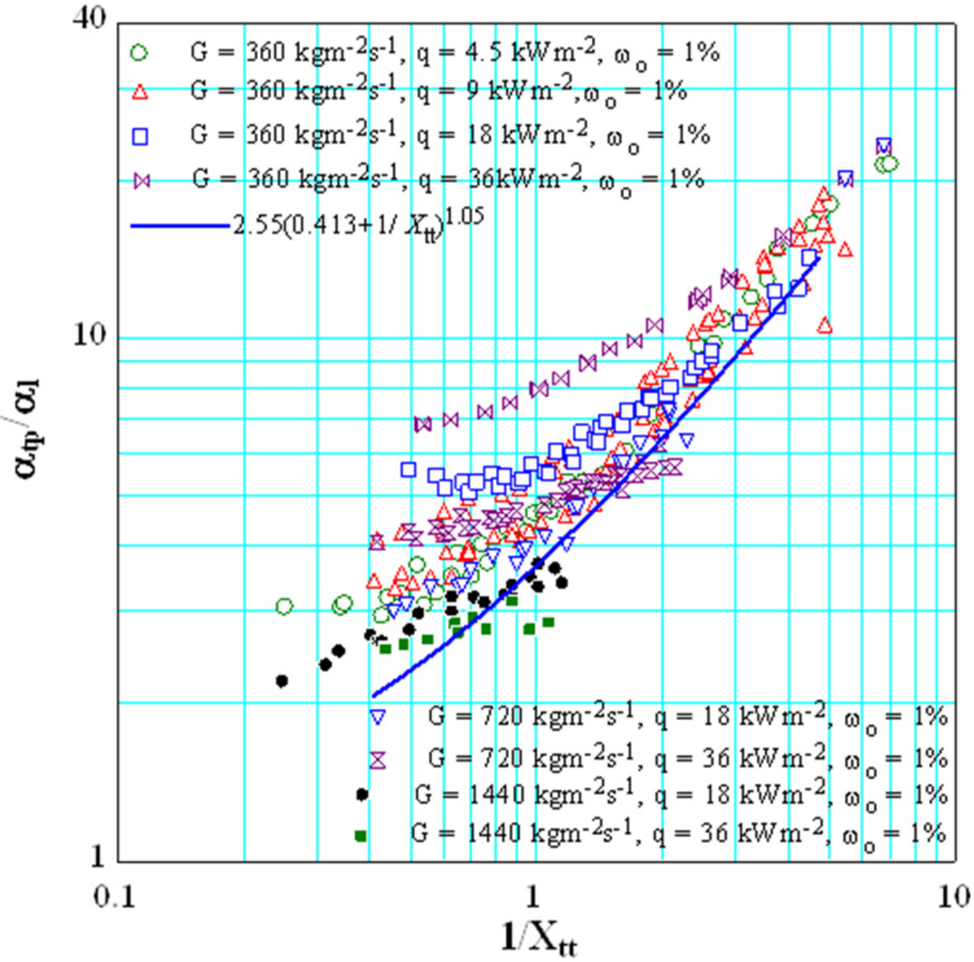

Figure 5 Variation in boiling heat transfer coefficient ratio against Lockhart–Martinelli parameter at ω_o = 1%.

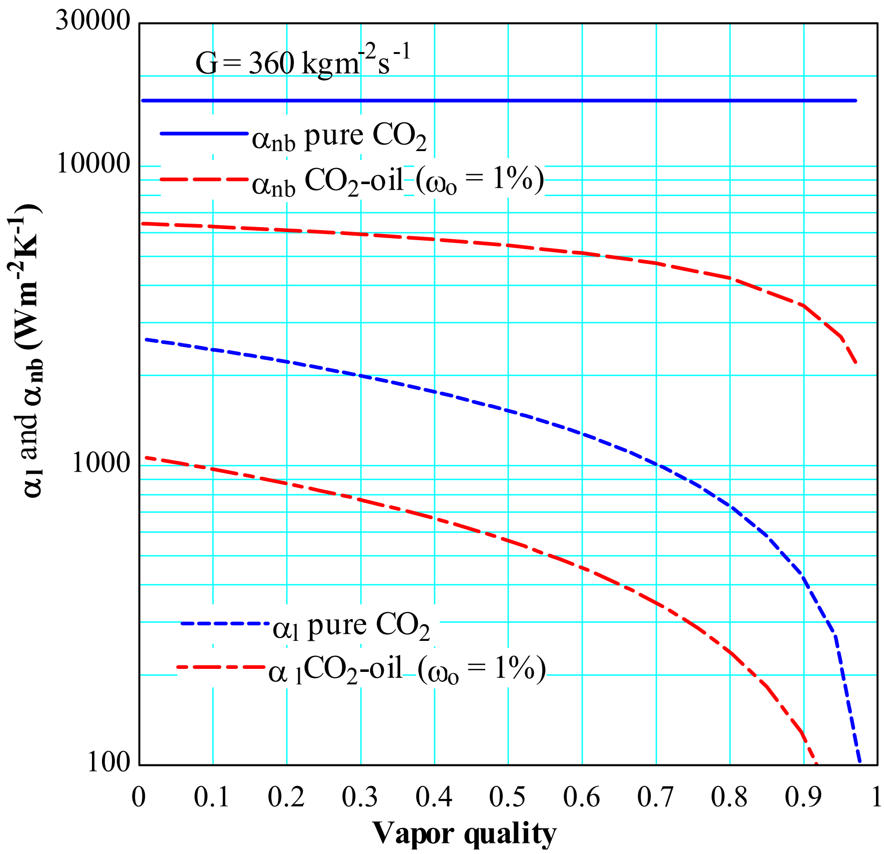

Figure 6 Comparison of α_l and α_{nb} calculated for pure CO_2 and for CO_2–oil.

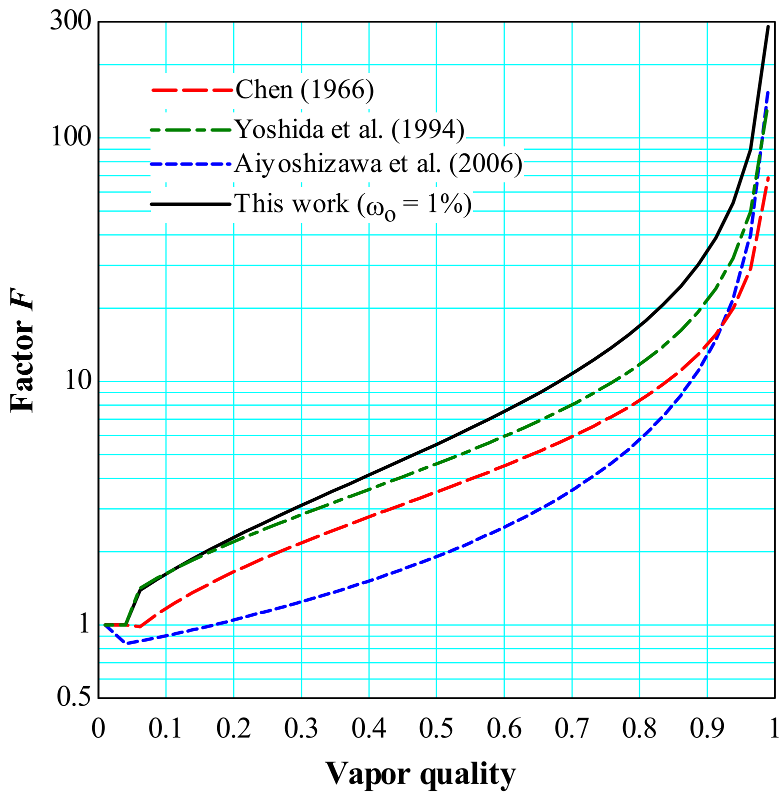

Figure 7 Variations in factor F values of four correlations at 15 °C against vapor quality.

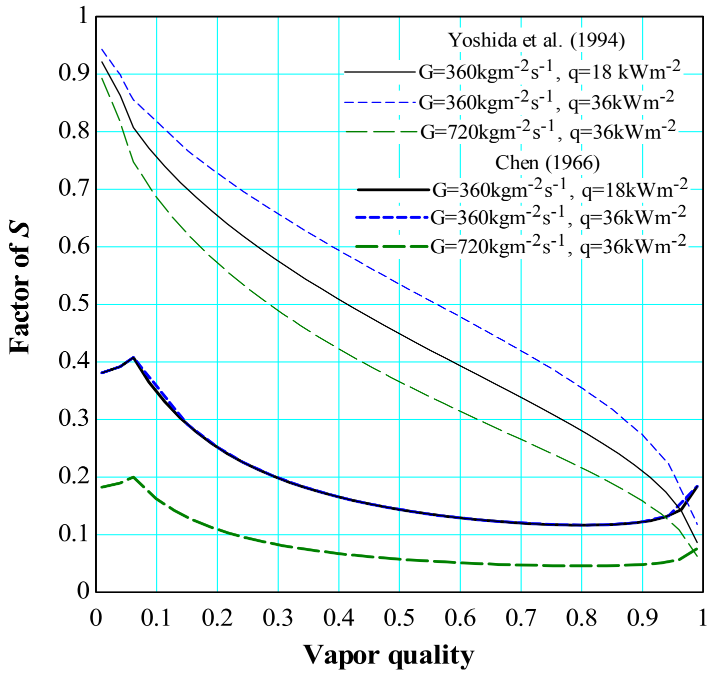

Fig. 8(a)

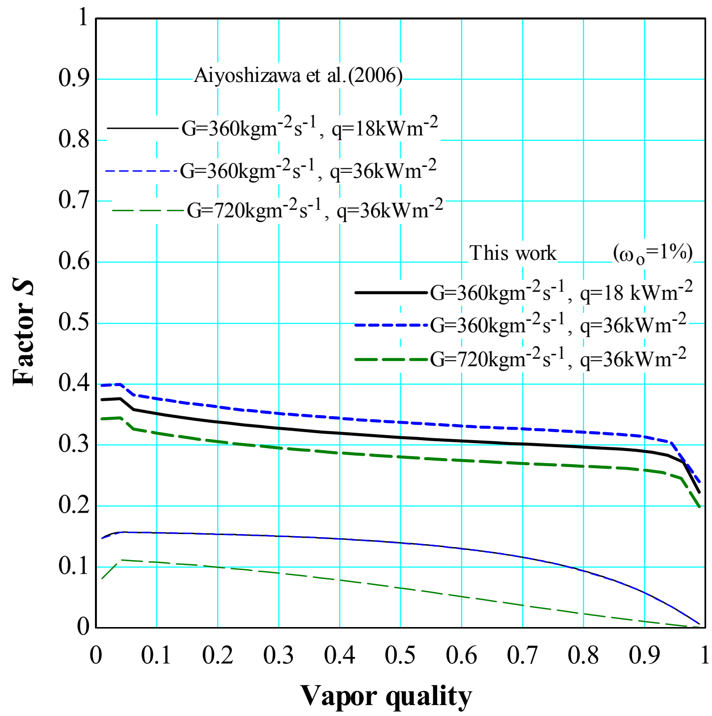

Fig. 8(b)

Figure 8 Variations in factor *S* values of four correlations at different mass and heat fluxes against vapor quality.

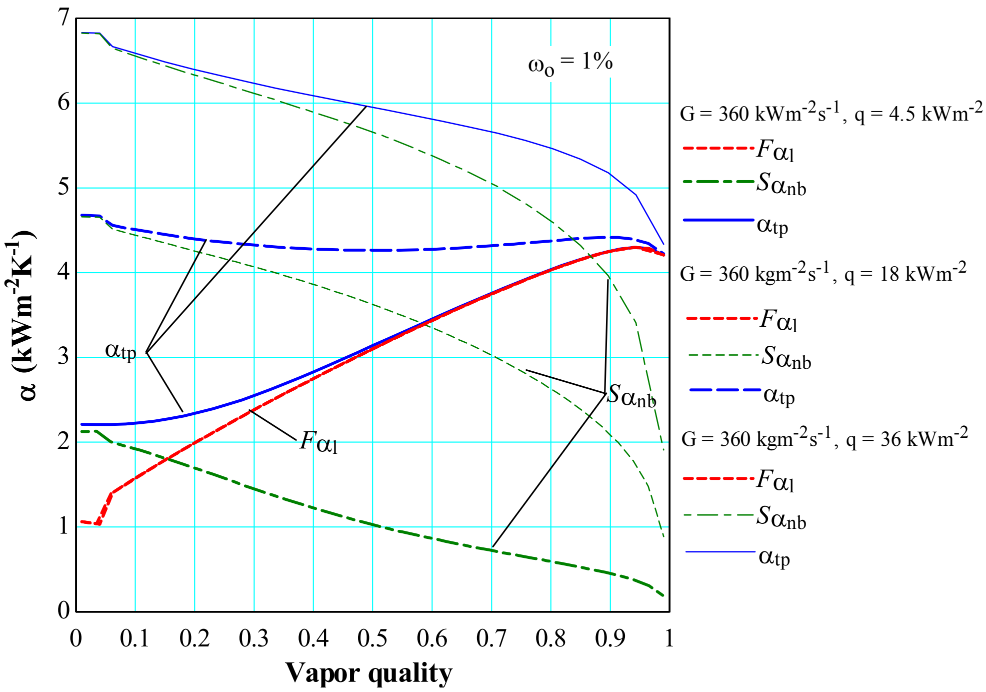

Figure 9 Contributions of different constituent terms to variation in total heat transfer coefficient (α_{tp}) from nucleate boiling ($S\alpha_{nb}$) and convective heat transfer ($F\alpha_l$) with the vapor quality

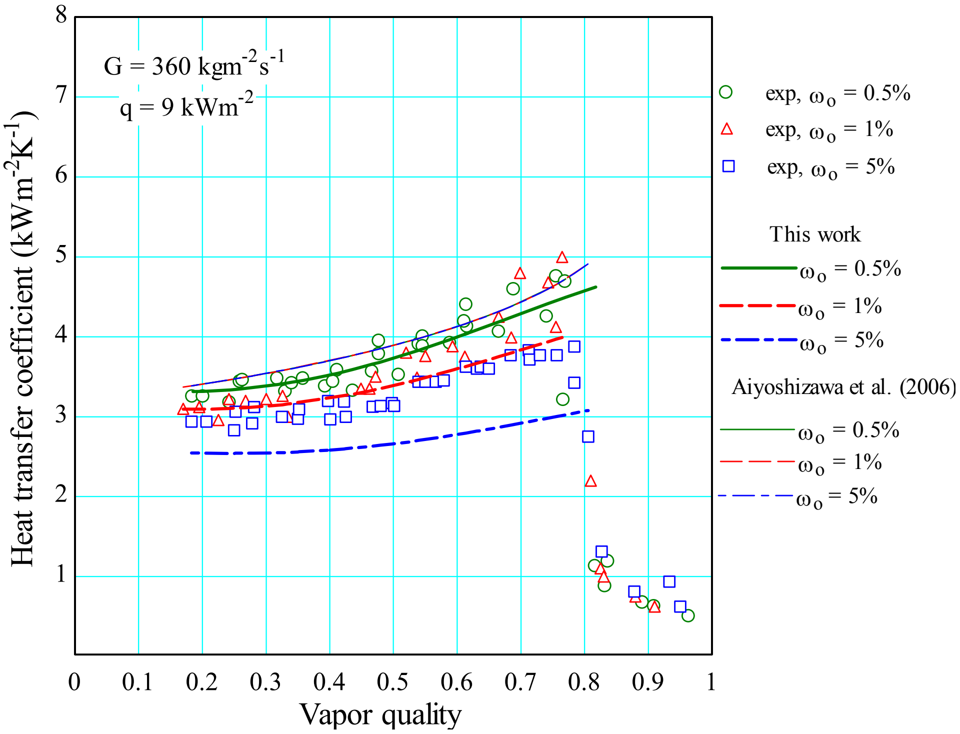

Fig. 10 (a) Data of Dang *et al*. (2013)

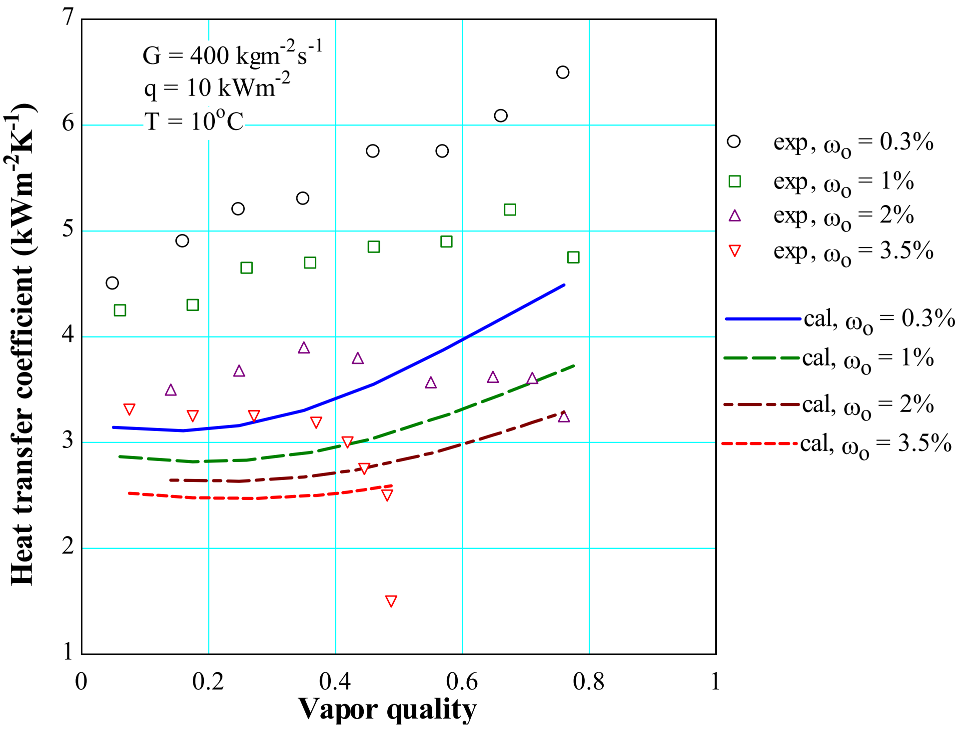

Fig. 10 (b) Data of Katsuta *et al*. (2008a)

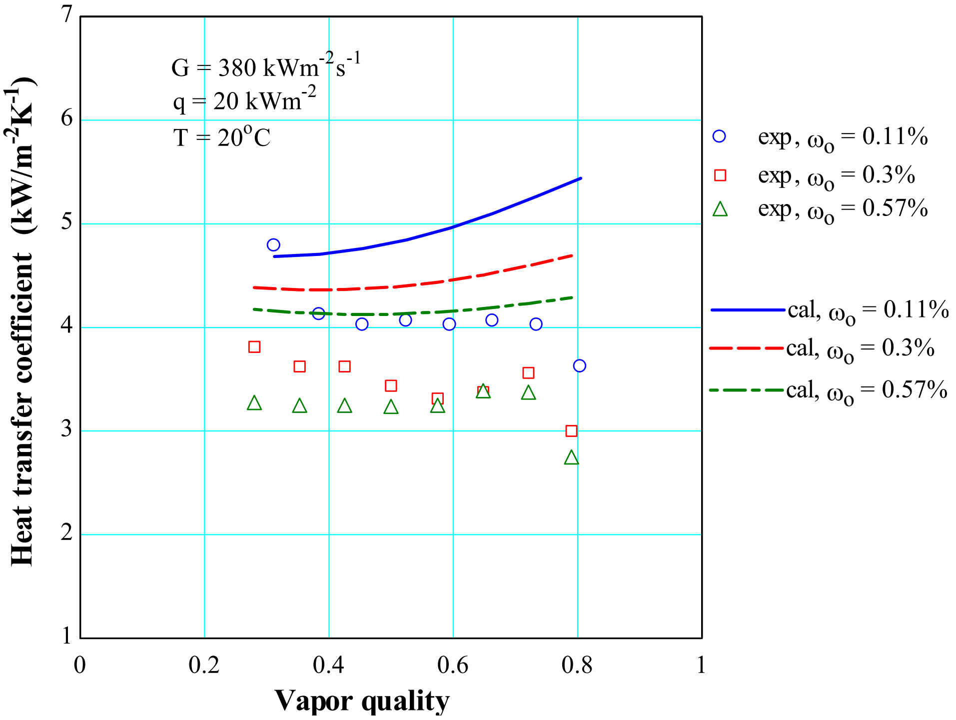

Fig. 10 (c) Data of Gao *et al*. (2007)

Figure 10 Comparison of measured heat transfer coefficients and those calculated using proposed correlation at different oil concentrations.

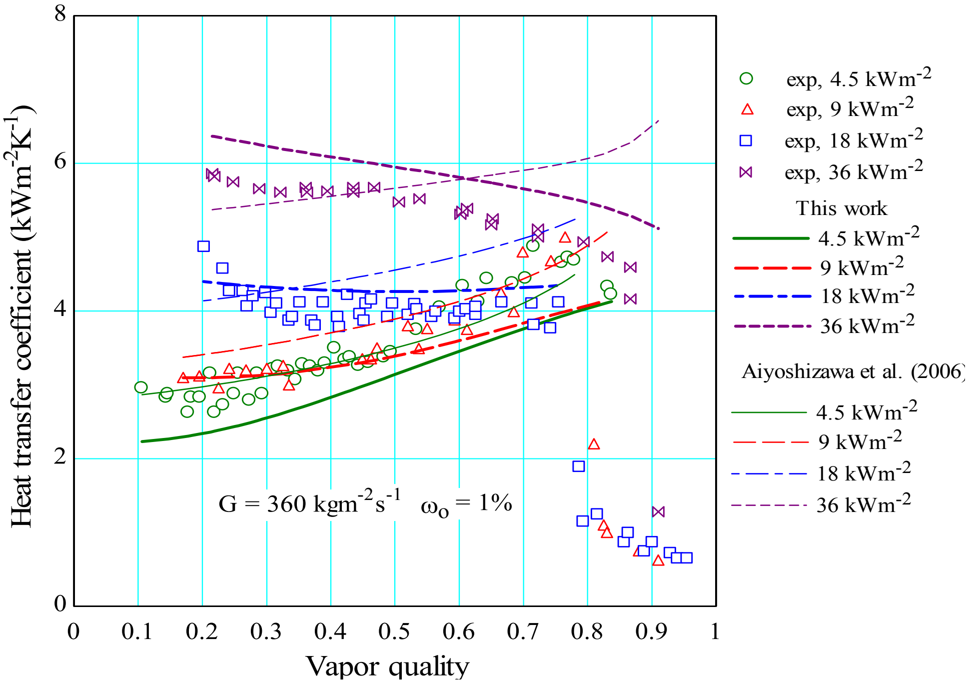

Fig. 11 (a) Various heat fluxes and constant mass flux

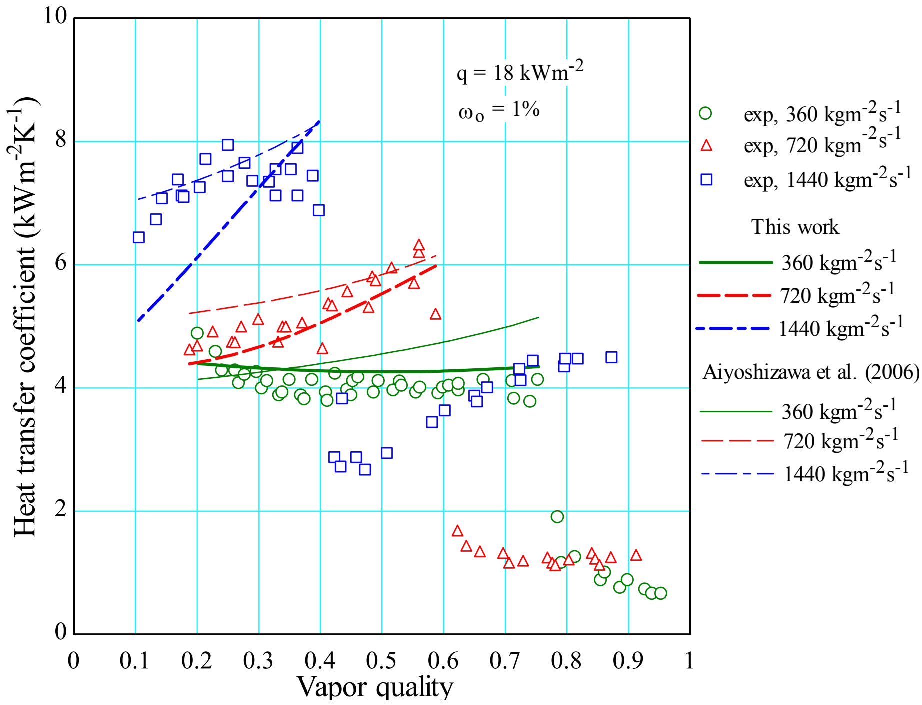

Fig. 11 (b) Various mass fluxes and constant heat flux

Figure 11 Comparison of theoretical heat transfer coefficients based on correlations of authors and Aiyoshizawa *et al*. (2006) and measured data in 2-mm I.D. tube at different mass and heat fluxes based on data of Dang *et al*. (2013).

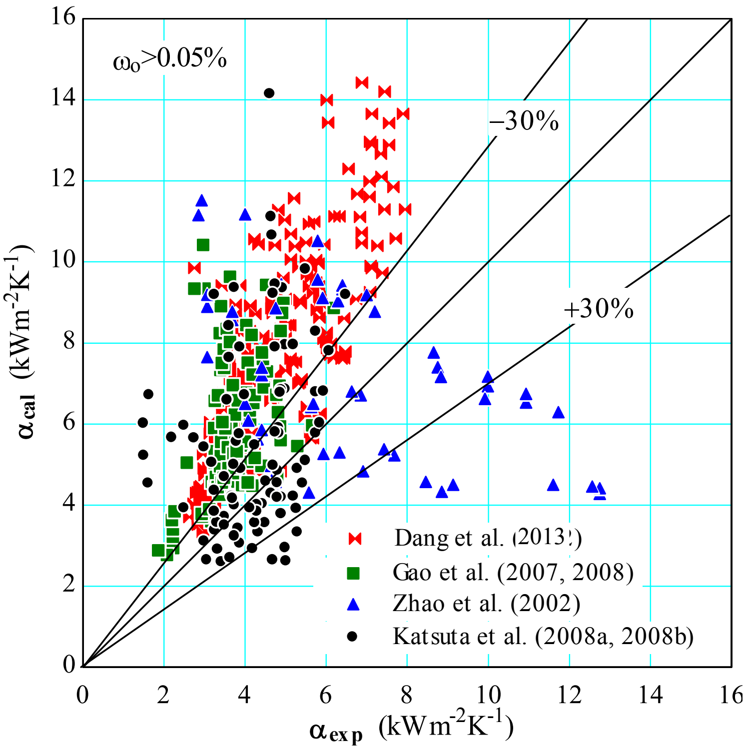

Fig. 12 (a) Correlations proposed by Gao *et al*. (2008)

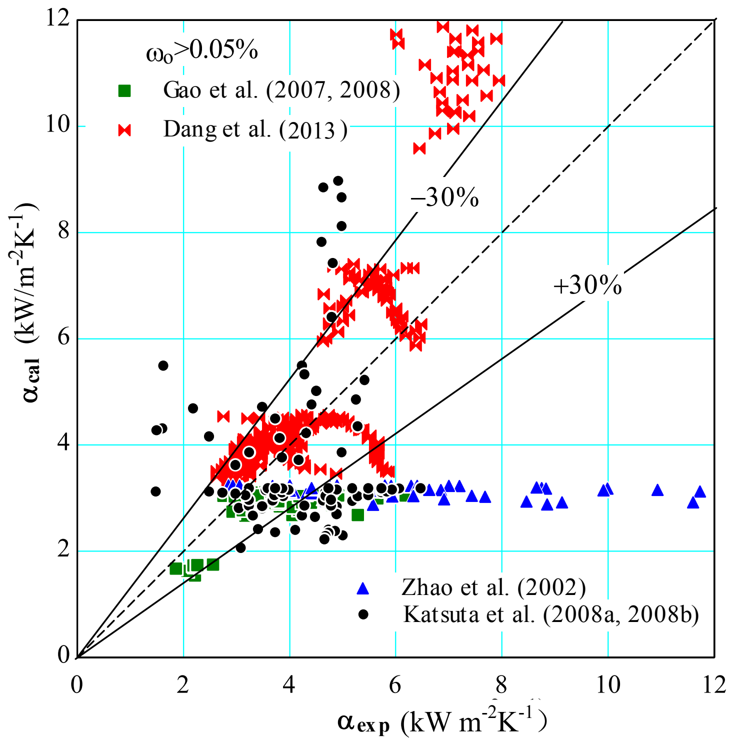

Fig. 12 (b) Correlations proposed by Katsuta *et al*. (2008)

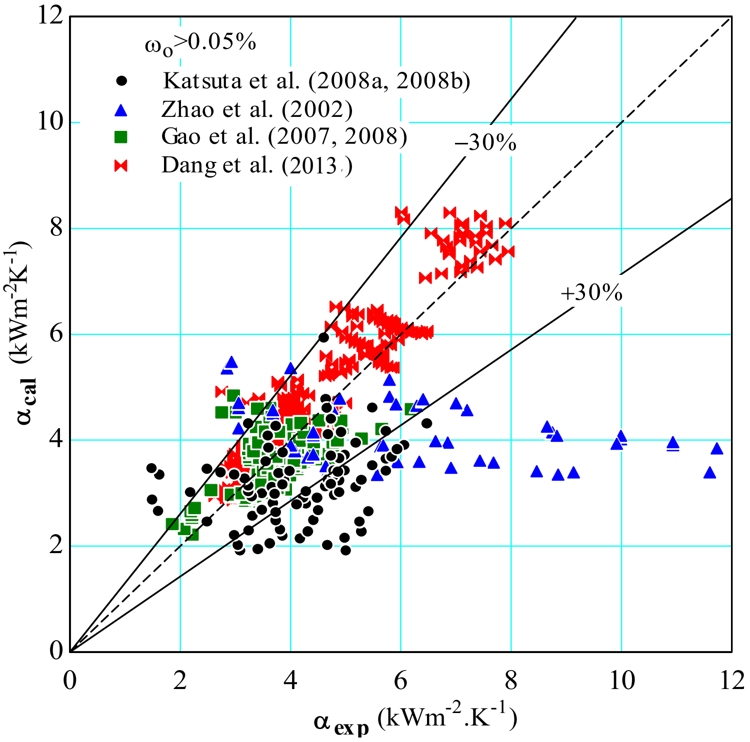

Fig. 12 (c) Correlations proposed by Aiyoshizawa *et al.* (2006)

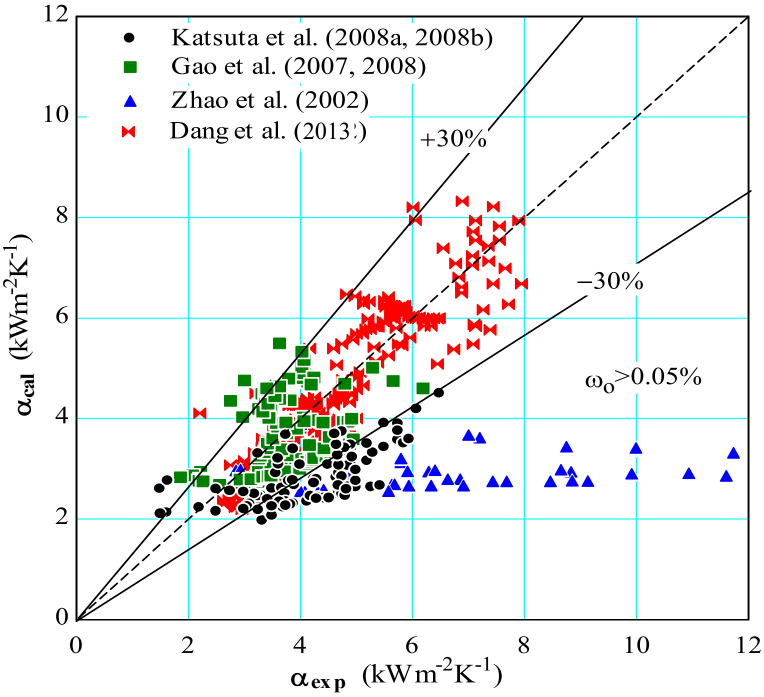

Fig. 12 (d) New correlations proposed by authors

Figure 12 Comparison of heat transfer coefficients predicted using six correlations and database.

Table 1 Experimental conditions

Tube Material	SUS316
Tube I.D. [mm]	2.0
Oil type	PAG100
Oil concentration [%]	0.5–5.0
Mass velocity [kg m^{-2} s^{-1}]	360, 720, 1440
Heat flux [kW m^{-2}]	4.5, 9, 18, 36
Evaporating temperature [°C]	15
Quality	Approximately 0–1.0

Table 2 Properties of PAG-type oil

Temperature [°C]	0	15	40	50	100
Molecular weight [kg $kmol^{-1}$]			1600		
Density	---	1000.6	---	1028.6	---
Specific heat [kJ kg^{-1} K^{-1}]	1.7577	---	---	1.9251	2.0925
Conductivity [W $m^{-1}K^{-1}$]	0.1478	---	---	0.1465	
Kinematic viscosity [mm^2 s^{-1}]	---	---	106.1	---	20.29
Standard boiling point [K]			845.41		
Critical temperature [K]			968.57		
Eccentricity factor			1.352		

Table 3 Comparison of the properties of the oil–CO_2 mixture and pure CO_2

Items	CO_2–oil mixture		oil	Pure CO_2
	1 % oil	5% oil		
Liquid conductivity [W m^{-1} k^{-1}]	0.09195	0.09355	0.1232	0.09186
Liquid viscosity [Pa s^{-1}]	7.35×10^{-4}	12.56×10^{-4}	3.41×10^{-3}	7.44×10^{-5}
Liquid density [kg m^{-3}]	822.73	828.85	1006.84	821.21
Specific heat [J kg^{-1} K^{-1}]	3425.16	3356.61	1728.58	3442.3
Surface tension [N m^{-1}]	0.00422	0.00701	0.0245	0.00196

The saturation temperature of pure CO_2 is 15 °C

Table 4 Experimental studies on flow heat transfer of CO_2–oil mixtures

References	Tube Inner D (mm), L (m)	Heat flux (kW m^{-2})	Mass flux (kg m^{-2} s^{-1})	Oil concentration (%)	Oil test methods	Saturated temperature (°C)	Number of data items $\omega_o > 0.05\%$
Katsuta *et al*. (2008a)	Smooth stainless D = 3 mm, L = 0.5 m	5, 10, 15 Electric heating	400	PAG 100, 0%, 0.05%–0.5%, 0.6%–1.2%, 1.8%–2.5%, 3.0%–4.0%	Oil supply system, oil mass flow meter, and oil sampling tank	–10, 0, 10	55
Katsuta *et al*. (2008b)	Smooth stainless D = 3 mm, L = 0.5 m	10 Electric heating	200, 400, 600	PAG 0%–0.05%, 0.5%–1.0%, 1.0%–2.0%, 2.0%–3.0%, 3.0%–5.0%, 7.0%–9.0%		0	34
Gao *et al*. (2008)	Smooth stainless inner D = 3.76 mm	10, 20, 30 Electric heating	100, 190, 380	PAG 1.01% PAG < 0.01%, 0.09%, 0.17%, 0.48%, 0.72%	Measured from the size and time interval of an oil droplet falling into the sight glass chamber	10	51
Gao *et al*. (2007)	Smooth stainless D = 3 mm, L = 2.185 m; Micro-fin D = 3.04 mm, Fin height = 0.11 mm	5, 10, 20, 30 Electric heating	190, 380, 770, 390, 780, 1180	PAG 0.01%, 0.11%, 0.30%, 0.57%		10	53
Zhao *et al*. (2002)	Mini tube D = 0.86 mm	11	300	Oil type N/A 0%, 1%, 3%, 4%, 5%, 7%	N/A	10	54
Dang *et al*. (2013)	Smooth stainless D = 2 mm	4.5, 9, 18, 36 Electric heating	360, 720, 1440	PAG 100, 0%, 1%, 3%, 5%	Oil sampling tube	15	274

Table 5 Deviations of methods when predicting heat transfer data at $\omega_o > 0.05\%$

Data / Model	Katsuta *et al*. (2008a, 2008b)		Zhao *et al*. (2002)		Dang *et al*. (2013)		Gao *et al*. (2007, 2008)	
	Mean absolute error	Standard deviation	Mean absolute error	Standard deviation	Mean absolute error	Standard deviation	Mean absolute error	Standard deviation
Thome *et al*. (2004)	–146%	290%	–141%	255%	194%	400%	196%	399%
Hwang *et al*. (1997)	63%	136%	32%	57%	123%	243%	109%	234%
Katsuta *et al*. (2008a)	42%	25%	46%	24%	21%	39%	21%	11%
Gao *et al*. (2008)	53%	112%	61%	118%	62%	129%	64%	141%
Aiyoshizawa *et al*. (2006)	32%	21%	40%	22%	10%	9%	14%	11%
This work	32%	13%	49%	20%	10%	7%	17%	10%